Phase separation in binary mixtures confined in a strip geometry

Aniket Bhattacharya,[1] Madan Rao,[2,3] and Amitabha Chakrabarti[3]
[1]*Department of Chemistry, Pennsylvania State University, University Park, Pennsylvania 16802*
[2]*Department of Physics, Indian Institute of Technology, Hauz Khas, New Delhi 110 016, India*
[3]*Department of Physics, Kansas State University, Manhattan, Kansas 66506*
(Received 14 July 1993)

We study the kinetics of phase separation of a model binary fluid confined within a narrow strip in two dimensions by numerically integrating the Cahn-Hilliard-Cook equation. We explore the systematics of the time evolution of domain shapes as a function of temperature and wetting field. The domains exhibit similar configurations as seen in recent Monte Carlo simulations of a related lattice model. We provide a quantitative estimate of the breakdown of power-law growth of domains once the domain size becomes comparable with the strip width, and show the relevance of the model to domain growth in Vycor glasses. Next we argue for the incorporation of an anisotropic kinetic coefficient in the coarse-grained dynamical equations. We find that even the slightest amount of anisotropy modifies the shapes of domains drastically and allows for complete phase separation.

PACS number(s): 47.55.Mh, 64.60.Cn, 68.45.Gd

I. INTRODUCTION

Binary fluid mixtures quenched inside their miscibility gap separate into two bulk coexisting phases. For a critical composition of the mixture, the phase separation is driven by small-amplitude long-wavelength fluctuations of the order parameter, known as spinodal decomposition. At late times a single length scale associated with the domain size governs the physics and the system enters a scaling regime [1].

Very different growth processes are observed during the phase separation of binary fluids in porous media such as Vycor glasses [2]. The two phases do not separate completely, even deep inside the coexistence region; instead, they form many microdomains, rich in either one phase or the other. While a complete theoretical understanding of this phenomenon is lacking, two very different interpretations have emerged so far. One is to map the phase separation of binary fluids in a porous medium onto the conserved dynamics of a random-field Ising model (RFIM) [3]. The slow dynamics is interpreted as arising from the random convolutions of the pore surface. A coarse-grained description in terms of the RFIM model would then predict that the length scale of the frozen microdomains is many times larger than the pore radius. Although qualitatively this model captures many features of slow kinetics and metastability, it has been recently criticized by Liu and co-workers [4–6]. They argue that the mapping onto the RFIM model is not appropriate for low-porosity media such as Vycor glasses (though it may possibly be applicable to high-porosity media such as silica gels) [6].

The alternate scenario proposed in Ref. [4] is that the metastability and slow kinetics of domain growth seen in experiments, originate not from the *random* convolutions of the pore surface but from the *geometric confinement* of the binary mixture inside the pores. To prove their point these authors investigate the dynamics of phase separation and wetting of the spin-exchange kinetic Ising (SEKI) model [6], confined within a single parallelepiped pore, using a Monte Carlo simulation. The equilibrium wetting "phase diagram" exhibits phases characterized by distinct shapes of the coexisting domains and separated by first-order boundaries. On quenching into any one of these two-phase regions, they find that as soon as the size of the evolving domains reaches the pore size, the growth towards equilibrium slows down drastically. However, a quantitative study detailing the growth kinetics for various quench temperatures and surface fields has not been undertaken.

In this paper we present a systematic investigation of the kinetics of domain growth of a model binary fluid confined to a single strip of finite width. The dynamics is modeled by a coarse-grained Cahn-Hilliard-Cook [1] equation which belongs to the same universality class as the SEKI model for bulk phase separation [7]. We also compare our results to a recent simulation of domain growth in a model porous medium in two dimensions [8] (which resembles a commercially prepared Vycor glass). This comparison is important since it is not *a priori* obvious that a single-pore model can do full justice to the very complex interconnections and the tortuous geometry of Vycor glasses.

We find that despite its simplicity, the coarse-grained model considered here captures the essential physics of phase separation in porous media. Our findings are in qualitative agreement with the results of Liu and coworkers and recent experiments [9] on phase separation of a binary mixture (polyvinyl methyl ether and water) confined in a capillary. As mentioned above, we actually go beyond these studies in providing quantitative estimates of the slow growth of domains. Comparison with the results of the computer simulation on phase separation in model Vycor glass lends strong support to the validity and the applicability of the single-pore model for a description of phase-separation processes inside porous glasses.

Finally, we incorporate an anisotropy in the kinetic coefficients entering into the dynamical equations dynamical equations. Though this anisotropy does not affect the asymptotic scaling behavior [10], it has a strong effect on the intermediate long-lived configurations that arose in our previous analysis. We find that even the slightest amount of anisotrpy promotes complete phase separation on time scales comparable to bulk phase separation times. We argue that this anisotropy in the kinetic coefficients originates from the anisotropic coarse-grained surface tension [10], which in turn, arises from the confining geometry.

The rest of the paper is organized as follows. In Sec. II we describe our model and the numerical procedure. In Sec. III we describe our results and compare them with previous simulation studies on microscopic Ising models. In Sec. IV we consider the effects of including an anisotropic kinetic coefficient in the coarse-grained model. Finally we conclude in Sec. V with a brief summary and discussion of the results.

II. MODEL AND NUMERICAL METHODS

We model the binary fluid by a coarse-grained order parameter $\phi(\mathbf{r},t)$, which is the difference in the concentrations of the two species α and β of the binary fluid, $\phi \equiv c_\alpha - c_\beta$. The binary fluid is confined in the $\hat{\mathbf{x}}$ direction ($\hat{\mathbf{y}}$ is along the impenetrable walls) to a strip of width L_x. The phenomenological Landau expansion [11] of the free energy of a binary system in this strip geometry is given by

$$\begin{aligned} F[\phi] &= F_{\text{bulk}} + F_{\text{surface}} \\ &= \tfrac{1}{2}\int dx\, dy \left[K|\nabla\phi|^2 - b\phi^2 + \frac{u}{2}\phi^4 \right] \\ &\quad + \int dy \{ \lambda^{-1}[\phi^2(x=0,y) + \phi^2(x=L_x,y)] \\ &\quad - h[\phi(x=0,y) + \phi(x=L_x,y)] \} \ . \end{aligned} \tag{1}$$

Since we will be interested in quenches below the bulk critical point, we have explicitly introduced a negative sign in the quadratic term in F_{bulk}. Moreover the coefficient K, related to the bare surface tension, has been chosen to be isotropic. We shall return to this point later in Sec. IV. The surface free energy consists of two parts—a surface-wetting field h, which favors the α component if $h > 0$, and a surface-enrichment (depletion) term $\lambda^{-1}\phi^2_{\text{surface}}$. The surface-wetting field h is taken to be short ranged and constant, acting only on the spins adjacent to the walls. The coefficient λ has the dimension of length and is called the *extrapolation length*. This Landau expansion is the continuum generalization of the lattice model studied by Monette, Liu, and Grest [6], with λ^{-1} proportional to the enhancement of exchange interactions in the surface layer J_1. Since in this study we are merely interested in the kinetics of phase separation between two bulk phases α and β, we henceforth set $\lambda^{-1}=0$ without any loss of generality. The ordering temperature T_c at $\lambda^{-1}=0$ turns out to be a *multicritical point* [12] and is called the *special transition*. The equilibrium mean-field equations obtained by a variation of the free-energy functional [Eq. (1)] is

$$-K\nabla^2\phi - b\phi + u\phi^3 = 0 \ , \tag{2}$$

which admits the natural boundary conditions

$$\left[\frac{\partial\phi}{\partial x} \right]_{x=0} = -h \ , \quad \left[\frac{\partial\phi}{\partial x} \right]_{x=L_x} = h \ . \tag{3}$$

We now quench a critical composition of the binary fluid from the infinite-temperature disordered phase through the special transition point into the two-phase coexistence region. Bulk phase separation proceeds in time, throughout which the composition is kept fixed. Thus the spatial integral of the order parameter is conserved and $\phi(\mathbf{r},t)$ evolves in time as

$$\frac{\partial\phi(\mathbf{r},t)}{\partial t} = M\nabla^2\mu + \eta(\mathbf{r},t) \ , \tag{4}$$

where μ is the local chemical potential, $\mu = \delta F/\delta\phi$, with F given by Eq. (1). The kinetic coefficient M is taken to be a constant, isotropic quantity. In Sec. IV we analyze the effect of introducing a small anisotropy in the kinetic coefficient. We note that in Eq. (4) $\phi(\mathbf{r},t)$ is coarse grained up to the bulk correlation length. The noise $\eta(\mathbf{r},t)$ is taken to be a Gaussian white noise with variance proportional to temperature T,

$$\langle \eta(\mathbf{r},t)\eta(\mathbf{r}',t') \rangle = -2k_B TM\nabla^2\delta(\mathbf{r}-\mathbf{r}')\delta(t-t') \ . \tag{5}$$

Before proceeding further,, we would like to remark that our analysis ignores the coupling of the order parameter to the momentum density of the fluid (hydrodynamics). This is an unjustified assumption and we hope to return to the full hydrodynamic problem in a future publication. Our study of domain growth is thus based solely on the evolution equation for the order parameter, Eq. (4). It is convenient to rescale variables

$$\frac{\mathbf{r}}{\sqrt{K/b}} \to \mathbf{r} \ , \quad \frac{t}{K/2Mb^2} \to t \ , \quad \frac{\phi}{\sqrt{b/u}} \to \phi \tag{6}$$

to obtain the simplified dimensionless equation

$$\frac{\partial\phi}{\partial t} = \tfrac{1}{2}\nabla^2(-\nabla^2\phi - \phi + \phi^3) + \sqrt{\epsilon}\xi \ . \tag{7}$$

The parameter ϵ is proportional to the temperature $\epsilon = k_B Tu/bK$ and the scaled Gaussian noise $\xi(\mathbf{r},t)$ satisfies

$$\langle \xi(\mathbf{r},t)\xi(\mathbf{r}',t') \rangle = -\nabla^2\delta(\mathbf{r}-\mathbf{r}')\delta(t-t') \ . \tag{8}$$

These dynamical equations should be supplemented by boundary conditions appropriate to the strip geometry. Since the walls at $x=0$ and L_x are impenetrable, global conservation of the order parameter would demand that no ϕ flux pass through it, so that

$$\left[\frac{\partial\mu(\mathbf{r},t)}{\partial x} \right]_{x=L_x;x=0} = 0 \ . \tag{9}$$

We also obtain a set of natural boundary conditions at the two walls which requires Eqs. (3) to hold at all times.

We impose periodic boundary conditions in the $\hat{y}$ direction.

At time $t=0$, we consider the critical mixture to be in equilibrium at $T=\infty$; this specifies an initial random configuration for $\phi(\mathbf{r},0)$. Equation (7) is then solved numerically on a two-dimensional square lattice of size $L_x \times L_y$ ($L_y \gg L_x$), where the spatial grid size $\delta r=1$. We use the standard Euler discretization with a time interval $\delta t=0.025$. This choice allows us to probe late times (up to $t_{mx}=10\,000$) for the system sizes we consider. In our simulations we take $L_y=100\delta r$ and $L_x=16\delta r$ or $32\delta r$. Our choice is consistent with typical values of pore size encountered in Vycor glass [13]—the pore diameter is roughly 60–70 Å, which is around 20 times the typical bulk correlation length.

We investigate the systematics of domain growth by quenching the system to various temperatures (ϵ) for different values of the surface-wetting field h. For each set of these parameters, we study the behavior of the order-parameter profile and correlation functions after averaging over 20 realizations of the initial configuration of the order parameter and thermal noise.

III. RESULTS

As we have mentioned before, we restrict our analysis to the case of a critical mixture where the volume fraction occupied by each component is exactly half. The equilibrium phase diagram (wetting diagram) has been extensively discussed by Liu *et al.* [4]. Even though their model is slightly different (see the discussion in Sec. II), the qualitative features of our phase diagram should be the same as theirs far below the critical (ordering) temperature. Since we have set $h>0$, the α component preferentially wets the walls; β is thus the nonwetting component. There are three distinct "phases" present in the wetting diagram exhibited by this model [4]; (i) the *tube*, where the α component forms a wetting layer of finite thickness and the β component is trapped in the middle in the form of a narrow strip. The α-β interface extends along the length of the strip; (ii) the *plug*, where the α and β components phase separate with the α-β interface across the strip; (iii) the *capsule*, a "shape transformation" from the tube state which comes about because of our constraint of fixed volume fraction and finite L_y. Here the α component wets the walls, but the β component gets trapped in the middle forming "bubbles" elongated along the strip. These "phases" are stabilized by an interplay between temperature-dependent surface tension and wetting forces. In our two-dimensional model, the wetting transition is continuous [14], while the shape transition between the tube and the capsule is first order.

Consider the time evolution of the order parameter during the spinodal decomposition process after a rapid quench into one of these equilibrium phases. For small surface wetting fields, the initial growth of domains might proceed unhampered as in the bulk, until the size of the growing domain is of the order of the strip width. The α-β interfaces of these domains are now across the strip, resembling a sequence of plug states. Each of these *mocroplugs* have roughly the same size, and the curvature of the interface is independent of their length; so the surface pressure for each will be the same. Subsequent growth by evaporation condensation (Ostwald ripening) slows down drastically. The motion of the interface is now along one dimension and so the kinetic coefficients get renormalized leading to nonalgebraic slow growth [15].

Though instantaneous snapshots of order parameter configurations at different times provide a useful representation of the kinetics [6], we have supplemented this information with more quantitative estimates of growth kinetics. We define the concentration profile ρ along the $\hat{\mathbf{x}}$ direction as

$$\rho(x_i,t)=\left\langle \sum_{j=1}^{L_y} \phi(x_i,y_j,t) \right\rangle , \tag{10}$$

where the averages are taken over different realizations of the initial configurations of the order parameter and thermal noise. The thickness of the wetting layer $l(t)$ can be obtained as the value of x where the concentration profile first goes to zero,

$$\rho[x=l(t),t]=0 . \tag{11}$$

We next define pair-correlation functions along the $\hat{\mathbf{x}}$ and $\hat{\mathbf{y}}$ directions. For example, along the $\hat{\mathbf{y}}$ direction, the pair-correlation function g_y is defined as

$$g_y(y,t)=\frac{1}{L_x}\sum_{i=1}^{L_x} g_{yi}(y,t) , \tag{12}$$

where $g_{yi}(y,t)$ is defined as

$$g_{yi}(y,t)=\left\langle \sum_j \phi[\mathbf{r}=(i,j),t]\phi[\mathbf{r}'=(i,j+y),t] \right\rangle . \tag{13}$$

A similar expression can be written for the pair-correlation function $g_x(x,t)$. The locations of the first zeros of these functions are taken as measures of average domain size $R_x(t)$ and $R_y(t)$ along the $\hat{\mathbf{x}}$ and $\hat{\mathbf{y}}$ directions, respectively. Due to the periodic boundary condition in the $\hat{\mathbf{y}}$ direction and the presence of the impenetrable walls in the $\hat{\mathbf{x}}$ direction, the correlations functions are computed for maximum separations of $L_y/2$ and $L_x/2$, respectively.

We will now describe our results for two values of the surface-wetting field h—a "weak" field, where the value of h in units of the surface tension (which in our rescaled variables is unity) is much smaller than 1, and a "strong" field, where $h\sim O(1)$, at various quench temperatures.

A. Weak surface field

We fix the surface field to be much smaller than the surface tension ($h=0.1$) and study the dynamics following temperature quenches deep in the two-phase region, $\epsilon=0.1$ and 0.5 (note that the bulk critical temperature $\epsilon_c \approx 0.75$ [16]). The equilibrium phase for these values of ϵ and h corresponds to the "plug" phase, with neither component preferentially wetting the walls. Do we reach this equilibrium phase at late times? Figure 1(a) shows a

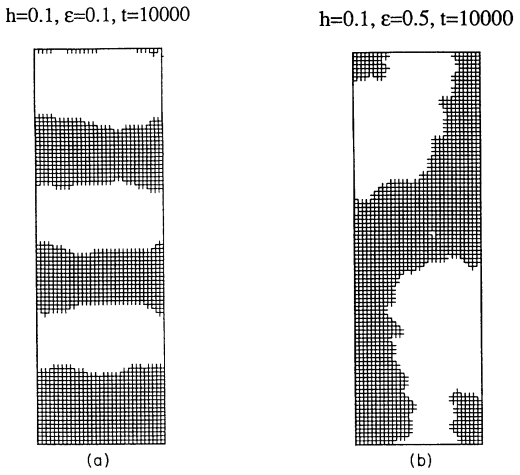

FIG. 1. (a) A typical configuration of the system at $t=10\,000$ for $h=0.1$, and $\epsilon=0.1$. Note the formation of the microplugs which make the evolution of the system extremely slow. (b) Same as in (a), with $\epsilon=0.5$. At this higher temperature, thermal fluctuations make the α-β interface of the microplugs wander, giving it curvature and promoting further, albeit slow growth.

typical configuration snapshot at a time as late as $t=10\,000$ for the lower temperature $\epsilon=0.1$. We see that microplugs, whose dimensions are of the order of the pore size, preempt the formation of the equilibrium plug phase. Once formed, as discussed earlier, further growth stops, consistent with the flatness of the α-β interface. At a higher temperature $\epsilon=0.5$, thermal fluctuations make the α-β interface of the microplugs wander, giving it curvature and promoting further, albeit slow growth [Fig. 1(b)].

In Figs. 2(a) and 2(b) we show the concentration profiles, for $\epsilon=0.1$ and 0.5, respectively, at two different times. For the lower temperature and at early times the α component shows a tendency to wet the walls, which, however, gives way to the formation of microplugs at later times. Note the occurrence of short-lived secondary peaks in the concentration profile [Fig. 2(a)], which is considerably smoothened due to thermal fluctuations at higher values of ϵ [Fig. 2(b)].

In Figs. 3(a) and 3(b) we show log-log plots of the average domain size in both the $\hat{\mathbf{x}}$ and $\hat{\mathbf{y}}$ directions, R_x and R_y, versus time for $\epsilon=0.1$ and 0.5, respectively. For the lower temperature we find that R_x shows a power-law growth with an exponent of about 0.35, until it reaches its maximal value equal to half the pore size. Though this is comparable to the $t^{1/3}$ growth, we would hesitate to associate this with the asymptotic Lifshitz-Slyozov behavior, since clearly we do not reach the asymptotic scaling regime. On the other hand, $R_y(t)$ [Fig. 3(a)] slows down considerably as soon as R_x reaches the size of the pore. This is due to the breakdown of the Ostwald ripening mechanism mentioned earlier. For the higher temperature, the domain size grows as shown in Fig. 3(b). Large thermal fluctuations make these data very noisy even after the averaging. We find that both R_x and R_y

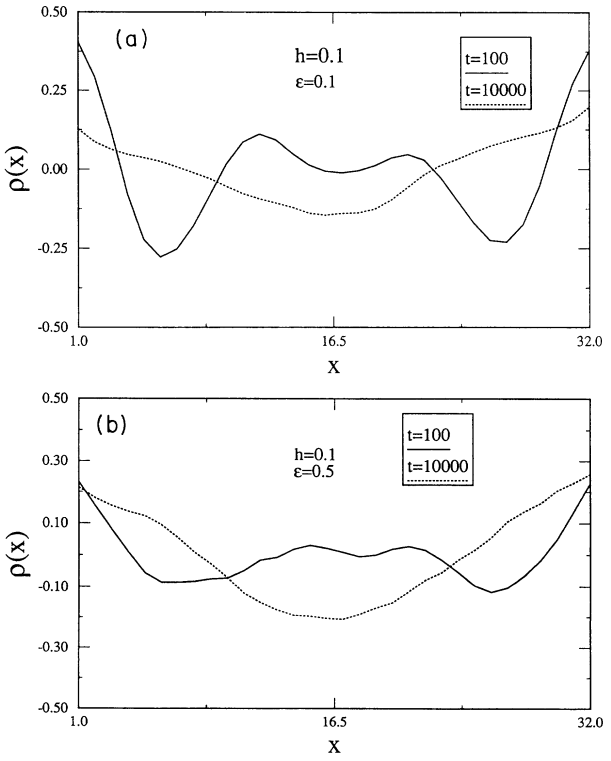

FIG. 2. (a) Density profiles for $h=0.1$, and $\epsilon=0.1$ for $t=100$, and $t=10\,000$. (b) Same as in (a), with $\epsilon=0.5$.

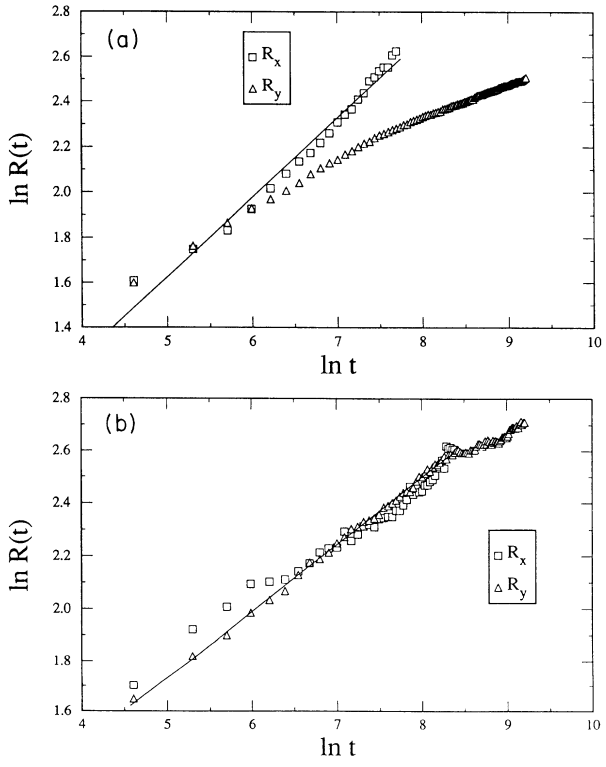

FIG. 3. (a) Log-log plot of the average domain size in the $\hat{\mathbf{x}}$ and $\hat{\mathbf{y}}$ directions with time for $h=0.1$. The straight-line fit yields an exponent of about 0.35. (b) Same as in (a), with $\epsilon=0.5$. The straight-line fit yields an exponent of about 0.25.

are quite similar to each other, until R_x is equal to the pore size, after which the growth of R_y slows down. The straight line fit to the data yields an exponent of 0.25, instead of the asymptotic exponent of $\frac{1}{3}$. As in Ref. [17], we note that for large noise strengths, the asymptotic scaling regime is numerically inaccessible.

B. Strong surface field

We now fix the surface field to be of the order of the surface tension ($h=1.0$) and again study domain growth at $\epsilon=0.1$ and 0.5. At equilibrium, the α component forms a thin wetting layer at the walls; the equilibrium phase corresponds to the tube. Even at very low temperatures, the evolution towards this equilibrium phase proceeds without any intervening long-lived microplugs [Figs. 4(a) and 4(b)]. However, at early times [Fig. 4(a)], we see the appearance of a secondary tube structure in the configuration, which disappears at late times. At higher temperatures the α-β interface fluctuations are enhanced [Fig. 4(c)].

The concentration profiles in Figs. 5(a) and 5(b) at the two temperatures reflect the configuration snapshots shown earlier. The sharpness of the drop in the concentration (at late times) away from the walls at lower temperatures is a restatement of the flatness of the α-β interface [Fig. 4(b)]. The profile, Fig. 5(a), shows an early time concentration banding induced by the wall potential. This is also seen in the configuration snapshots, Fig. 4(a) (although at a later time). We note that such concentration banding (or the so-called spinodal wave) in the presence of one wetting surface [18,19] and interference of the spinodal waves in the presence of two opposing walls [20] have been studied extensively in recent theoretical and experimental work. The high cost in interfacial energy disrupts these bands leading to eventual thermal equilibrium.

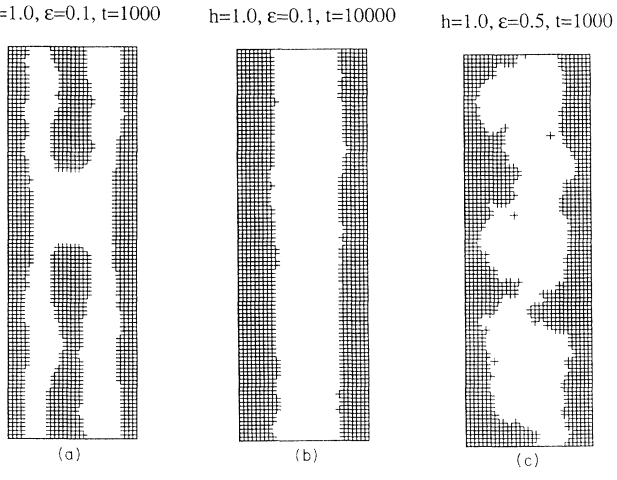

FIG. 4. (a) A typical configuration of the system at $t=1000$ for $t=1.0$, and for $\epsilon=0.1$. Note the formation of the secondary structure in the middle. (b) Same as in (a), at $t=10\,000$. The secondary structure has disappeared and a final tube structure is clear. (c) Same as in (a), with $\epsilon=0.5$. Once again we see a tube structure, but at this higher temperature, thermal fluctuations make the α-β interface quite rough.

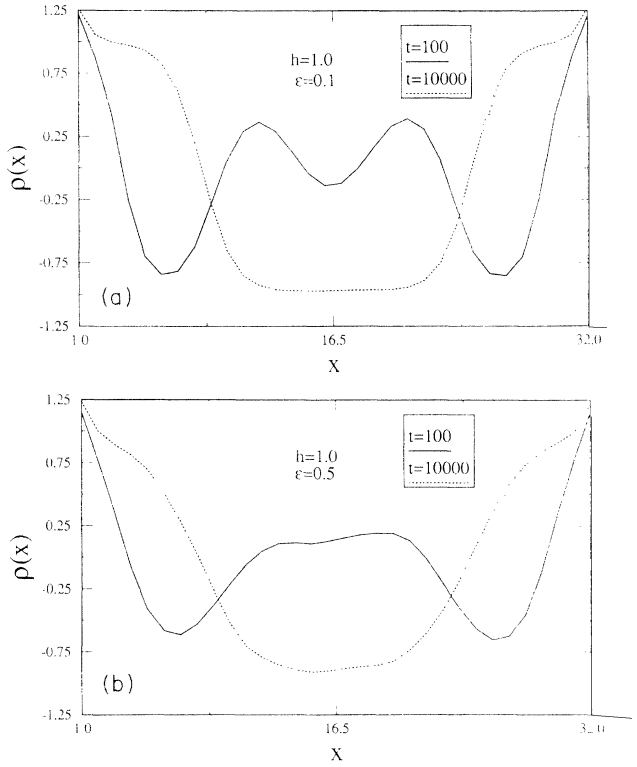

FIG. 5. (a) Density profiles for $h=1.0$, and $\epsilon=0.1$ for $t=100$, and $t=10\,000$. (b) Same as in (a), with $\epsilon=0.5$.

C. Comparison with phase separation in model Vycor glass

In Ref. [8], a model Vycor glass was prepared by quenching a model binary mixture down to zero temperature. At a suitable intermediate time, the growth was halted and one of the components was numerically "etched out." The resulting configuration snapshot is a good imitation Vycor glass. Chakrabarti [8] then studied the phase separation kinetics of a binary fluid confined within this Vycor glass. As in this study, he found that the crossover to slow growth (discussed in Sec. III A) occurs when the domain size gets to be of the order of the pore size r_0. The persistence length l of the pores is a good measure of the length scale over which pores curve. If $l \gg r_0$, then the single pore description should be adequate to describe this slow dynamics. In some experiments [13], however, $l=45$ Å, while the average pore size is $r_0=35$ Å; in such cases the curvature of the caps of the microplugs would depend on the curvature of the pore surface and the crossover to slow growth might happen at a slightly larger length scale than the pore radius.

IV. EFFECTS OF ANISOTROPIC KINETIC COEFFICIENT

We have noted in Sec. II that the coefficients of the nonlocal terms K (surface tension) and M (kinetic coefficient) in our coarse-grained model were taken to be

isotropic. Rotational invariance of the Hamiltonian and the corresponding Langevin equation in bulk systems would demand that both K and M be symmetric in the $\hat{\mathbf{x}}$ and $\hat{\mathbf{y}}$ directions, $K_x = K_y$ and $M_x = M_y$. This invariance is broken explicitly by the presence of the confining walls. Thus there is no reason for K and M to be the same in the two directions any more. This asymmetry is of course irrelevant to the asymptotic scaling behavior. In a renormalization-group sense, an isotropy in the surface tension and the kinetic coefficient (above the roughening temperature) is irrelevant [10] at the zero-temperature fixed point which governs the dynamics in the order phase. However, it can and does affect the early-time behavior. In the context of phase separation in a strip, it could lead to a faster initial growth of domains in the $\hat{\mathbf{y}}$ direction than in the $\hat{\mathbf{x}}$. Thus we would expect to see growing domains elongated in the $\hat{\mathbf{y}}$ direction which then merge with other domains leading to a complete phase separation. In this way, it might be possible to avoid the intermediate microplug configurations seen for small values of the wetting field at low temperatures.

To test this hypothesis we quench the system from the $T=\infty$ disordered phase to a zero-temperature ordered phase in the absence of any surface field. The equilibrium phase corresponds to a plug configuration. We have chosen the width of the strip $L_x = 16$. With the kinetic coefficients in the two directions being equal, the order parameter evolves according to Eq. (7). For small values of h (including $h=0$) and ϵ (including $\epsilon=0$), we find as before that the global equilibrium state is preempted by the formation of long-lived microplugs. We now introduce an asymmetry in M. The evolution equations for the order parameter (after rescaling) are now given by

$$\frac{\partial \phi(\mathbf{r},t)}{\partial t} = M_x \frac{\partial^2 \mu}{\partial x^2} + M_y \frac{\partial^2 \mu}{\partial y^2} + \eta(\mathbf{r},t) \ . \tag{14}$$

We have solved these equations as before, subject to the same boundary and initial conditions. For simplicity we consider $h=0$ and $\epsilon=0$. We find that, for an asymmetry ratio $R \equiv M_x/M_y \geq 1.035$, the system phase separates completely over time scales comparable to bulk separation time scales ($t_{\max} = 10\,000$). There are no intervening microplug configurations which would have prevented global phase separation. Let us denote by R_c the critical asymmetry ratio beyond which complete phase separation is obtained and analyze its dependence on the parameters of the model. For fixed h and ϵ, R_c clearly depends on L_x, the width of the strip, and decreases to unity as L_x increases. From our simulations done at various values of L_x ($L_x = 11$ to 16) and analytical arguments based on finite size scaling of the surface tension [21], we deduce that $R_c = 1 + A \exp(-BL_x^2)$, where A and B are some constants. Putting in experimentally relevant parameters [13] of $L_x = 20$ (in units of correlation length), we find that the asymmetry required for complete phase separation is less than 0.2%. This behavior is also seen in the presence of a weak surface field but still in the plug phase.

Having shown explicitly how a small amount of asymmetry in the kinetic coefficient may give rise to quite different phase separation kinetics, we will now try to explore the origins of such an asymmetry. Our arguments here will be purely heuristic; we leave detailed calculations for another publication [21]. The final content of the argument is the following: anisotropic surface tensions in the Hamiltonian lead to anisotropic kinetic coefficients in the Langevin equation. Restricting ourselves to the strip geometry, we see, following the work by Abraham, Svrakic, and Upton [22], that a bubble of the nonwet component possesses an interface more elongated along the $\hat{\mathbf{y}}$ direction than along the $\hat{\mathbf{x}}$. Thus the surface tension K_x normal to the elongated interface is smaller than K_y. An anisotropic square-gradient term in the continuum limit also arises if one considers an anisotropic bulk coupling in the original lattice theory [23]. Thus the presence of an anisotropic square-gradient term is expected if the interactions between the molecules are anisotropic.

Siegert [10] has demonstrated in the context of a nonconserved order parameter that the inclusion of an anisotropic surface tension in the Langevin equation reflects in an anisotropy in the kinetic coefficient when written in terms of interface variables. The anisotropic kinetic coefficient is inversely related to the anisotropic surface tension. Thus M_x should be larger than M_y. A similar analysis should hold even in the presence of a conservation law. That the kinetic coefficients should become anisotropic under renormalization is not surprising, since clearly the asymmetry in M_x and M_y should grow as the coarse-graining length scale gets to the order of the width of the strip. At this length scale, the dynamics becomes one dimensional and M_x goes to infinity while M_y gets renormalized to an exponential form leading to the logarithmically slow growth [15].

V. CONCLUSIONS

In summary, we have numerically studied a coarse-grained model of phase separation of binary fluids kept inside a two-dimensional strip geometry. Both the kinetics of domain growth and the equilibrium behavior of the binary mixture are investigated in this paper. In the first set of calculations, we have considered a constant, isotropic kinetic coefficient in our model calculations and applied various values of surface fields at the confining walls. In agreement with theoretical arguments and previous simulation results in a microscopic lattice model, we find that for small fields and low temperatures, the kinetics of domain growth becomes very slow due to the breakdown of Ostwald ripening mechanism, once the domain size becomes comparable to the pore radius. This leads to the formation of the long-lived *microplugs* and the system is not allowed to reach the equilibrium phase within any reasonable time scale. On the other hand, for strong values of the wetting field, the system forms the so-called *tube* configurations, and equilibrium is readily reached at all temperatures.

Next we considered the effect of a slight anisotropy in the kinetic coefficient on the phase-separation behavior.

We provided heuristic arguments of how such an anisotropy in the kinetic coefficient could arise due to an anisotropic surface tension originating from the confining geometry. We find that for fixed values of the wetting field and the temperature, there is a critical value of the anisotropy which allows complete phase separation avoiding the intervening microplug configurations. We have also computed how this critical value of the anisotropy depends on the strip width and find that for experimentally relevant situations, the anisotropy required for a complete phase separation is quite small, even at low temperatures.

ACKNOWLEDGMENTS

The work at Kansas State University has been supported by the National Science Foundation (Grant No. DMR-9312596). The computer calculations were carried out under a NSF grant of computer time from the Pittsburgh Supercomputing Center. A.B. thanks Professor J. B. Anderson and acknowledges support from NSF Grant No. CHE-8714613 and ONR Grant No. N00014-92-J1340.

[1] For a review, see J. D. Gunton, M. San Miguel, and P. S. Sahni, in *Phase Transitions and Critical Phenomena,* edited by C. Domb and J. L. Lebowitz (Academic, London, 1983), Vol. 8.

[2] See, for example, W. I. Goldburg, in *Dynamics of Ordering Processes in Condensed Matter,* edited by S. Komura and H. Furukawa (Plenum, New York, 1988).

[3] F. Brochard and P. G. de Gennes, J. Phys. Lett. (Paris) **44**, 785 (1983); P. G. de Gennes, J. Phys. Chem. **88**, 6469 (1984); D. Andelman and J. F. Joanny, in *Scaling Phenomena in Disordered Systems,* edited by R. Pynn and A. Skjeltorp (Plenum, New York, 1985).

[4] A. J. Liu, D. J. Durian, E. Herbolzheimer, and S. A. Safran, Phys. Rev. Lett. **65**, 1897 (1990).

[5] A. J. Liu and G. S. Grest, Phys. Rev. A **44**, R7879 (1991).

[6] L. Monnette, A. J. Liu, and G. S. Grest, Phys. Rev. A **46**, 7664 (1992).

[7] J. D. Gunton, E. T. Gawlinski, A. Chakrabarti, and K. Kaski, J. Appl. Cryst. **21**, 811 (1988).

[8] A. Chakrabarti, Phys. Rev. Lett. **69**, 1548 (1992).

[9] H. Tanaka, Phys. Rev. Lett. **70**, 53 (1993).

[10] M. Siegert, Phys. Rev. A **42**, 6268 (1990).

[11] For a review, see K. Binder, in *Phase Transitions and Critical Phenomena* (Ref. [1]).

[12] A. J. Bray and M. A. Moore, J. Phys. A **10**, 1927 (1977).

[13] P. Levitz and J. M. Drake, Phys. Rev. Lett. **58**, 686 (1987); P. Levitz, G. Ehret, S. K. Sinha, and J. M. Drake, J. Chem. Phys. **95**, 6151 (1991).

[14] See, for example, M. E. Fisher, in *Statistical Mechanics of Membranes and Surfaces,* Jerusalem Winter School for Theoretical Physics, edited by D. Nelson, T. Piran, and S. Weinberg (World Scientific, Singapore, 1987).

[15] K. Kawasaki and T. Ohta, Physica A **116**, 573 (1982); T. Kawakatsu and T. Munaka, Prog. Theor. Phys. **74**, 11 (1985).

[16] R. Toral and A. Chakrabarti, Phys. Rev. B **42**, 2445 (1990).

[17] T. M. Rogers, K. R. Elder, and R. C. Desai, Phys. Rev. B **37**, 9638 (1988); A. Chakrabarti (unpublished).

[18] R. C. Ball and R. L. H. Essery, J. Phys. Condens. Matter **2**, 10 303 (1990); G. Brown and A. Chakrabarti, Phys. Rev. A **46**, 4829 (1992); S. Puri and K. Binder, *ibid.* **46**, R4487 (1992); J. F. Marko, Phys. Rev. E **48**, 2861 (1993); W. J. Ma, P. Keblinski, A. Maritan, J. Koplik, and J. R. Banavar, *ibid.* **48**, R2362 (1993).

[19] R. A. L. Jones, L. J. Norton, E. J. Kramer, F. S. Bates, and P. Wiltzius, Phys. Rev. Lett. **66**, 1326 (1991); G. Krausch, C. Dai, E. J. Kramer, and F. S. Bates, Phys. Rev. Lett. **71**, 3669 (1993).

[20] G. Krausch, C. Dai, E. J. Kramer, J. F. Marko, and F. S. Bates (unpublished).

[21] M. Rao, Aniket Bhattacharya, and A. Chakrabarti (unpublished).

[22] D. B. Abraham, N. M. Svrakicc, and P. J. Upton, Phys. Rev. Lett. **68**, 423 (1992).

[23] H. Nakanishi and M. Fisher, J. Chem. Phys. **78**, 3284 (1983).